Computers and Electronics in Agriculture 82 (2012) 134–144

Contents lists available at SciVerse ScienceDirect

Computers and Electronics in Agriculture

journal homepage: www.elsevier.com/locate/compag

Software for the geometric characterisation of insect-proof screens

A.J. Álvarez *, R.M. Oliva, D.L. Valera

Departamento de Ingeniería Rural, Escuela Superior de Ingeniería, Universidad de Almería, 04120 Almería, Spain

ARTICLE INFO

Article history:
Received 2 June 2011
Received in revised form 27 December 2011
Accepted 2 January 2012

Keywords:
Insect-proof screens
Geometric characterisation
Software development
Image analysis

ABSTRACT

Novel software has been developed for the geometric characterisation of agrotextiles intended for installation in greenhouse vents as a means of crop protection. This characterisation of insect-proof screens is essential with a view to keeping insects out and also from an aerodynamic point of view. The method of analysis is based on digital images taken by microscope or scanner. The geometric procedure considers that each hole of the screen represents a quadrilateral, as it is defined by four threads of monofilament that cross over each other. The software developed using Visual Basic allows us to identify the coordinates of the vertices of the quadrilaterals and therefore to carry out a complete characterisation of the agrotextiles: number of threads per unit length, porosity of the sample, dimensions of the holes, thickness of the threads, area of the holes and the largest circle contained in the holes. The analysis of the data provided by the software allows us to study the uniformity of the material and also to detect flaws in its manufacture. The software includes a pattern for identifying the vertices with a high percentage of accuracy. For instance, it analysed over 40,000 vertices with only 1.14% error, mostly due to dirt on the screen. The software developed includes procedures to detect these errors, to alert the user to the type of error and to correct them. There is no other specific procedure to measure the characteristic dimensions of insect-proof screens and, therefore, it is no possible to contrast in this way the results that are obtained with the proposed method. Consequently, the measurement method has been verified using a set of screens of known dimensions manufactured for this very purpose. The results obtained are excellent, revealing that the differences between the expected values and the measured ones are well below the sensitivity of the device used to obtain the digital images.

1. Introduction

Insect-proof screens are a physical means of crop protection whose use has become widespread in many parts of the world over recent decades. They are installed at the side and roof vents of greenhouses with a view to impeding or reducing the access of insects to the crop. Different species of aphids, whitefly, thrips and leafminers are among the most damaging pests for greenhouse crops (Hussey, 1985). They not only produce direct damage by feeding and laying eggs, they also transmit phytopathogenic organisms (Smith, 1972; McLean et al., 1986). Indeed, in certain cases, this is of much greater concern to growers than the direct damage they cause (Brown and Brown, 1992; Lacasa and Contreras, 1993).

Obtaining the geometric characteristics of insect-proof screens is of great interest from different perspectives as it is the starting point for work related to crop protection and research whose aim consists of determining the reduction of airflow caused by the screen (influence on the ventilation and the microclimate). Therefore, the quality of the results obtained by researchers in their work is affected by the accuracy of the data related to the geometry of the screen. The published articles usually do not describe the method of measurement used in determining the dimensions of the screen. Despite the importance exposed, nowadays there is no method that is designed to give a specific solution to this problem. The data shown in the research literature may have been obtained using generic programmes provided for the handling of certain devices (microscopes, scanners) and which allow measurements by clicking on the images obtained. Obviously, such measurements are inaccurate and require a substantial amount of time to obtain a small number of data (just imagine how slow and inaccurate that it is to get the dimensions of a single hole, for example the length of the hole by clicking with the mouse button at the point of origin and end of the segment that defines this dimension). There are other generic programmes that can segment the image into objects and background and obtain measurements of the objects identified; however, the general nature of these programmes means that the solutions they provide do not solve the specificity of the problem posed in this work.

The structure of the weave of insect-proof screens is determined by two sets of threads (weft and warp) which interweave perpendicularly. The separation of the threads in each direction

* Corresponding author. Tel.: +34 950015825; fax: +34 950015491.
E-mail address: ajalvare@ual.es (A.J. Álvarez).

0168-1699/$ - see front matter © 2012 Elsevier B.V. All rights reserved.
doi:10.1016/j.compag.2012.01.001

Nomenclature

A, B, C, D	vertices of a quadrilateral
AC	straight line that includes the vertices A and C
A_p	porous surface area (m^2)
A_t	total surface area (m^2)
d	distance between centre of a circle and a side of quadrilateral (m)
D_{hx}	thickness of the weft threads (m)
d_{hx}	mean thickness of the weft thread measured in the direction of the lines that include points $R_{(1,j)}$ and $S_{(m,j)}$ (m)
D_{hy}	thickness of warp threads (m)
d_{hy}	mean thickness of the warp thread measured in the direction of the lines that include points $P_{(i,1)}$ and $Q_{(i,n)}$ (m)
L_{B-AC}	distance between the vertex B and the straight line AC (m)
L_{D-AC}	distance between the vertex D and the straight line AC (m)
L_{PQ}	distance between points P and Q (m)
L_{px}	mesh size measured in the weft direction (m)
l_{px}	mean mesh size measured in the direction of the lines that include $P_{(i,1)}$ and $Q_{(i,n)}$ (m)
L_{py}	mesh size measured in the warp direction (m)
l_{py}	mean mesh size measured in the direction of the lines that include $R_{(1,j)}$ and $S_{(m,j)}$ (m)
m_{AC}	slope of the straight line AC
n_{AC}	y-intercept of the straight line AC
O_1	centre of the circle (m)
P	midpoint located between the vertices A and B
Q	midpoint located between the vertices C and D
R	midpoint located between the vertices B and C
r	radius of the circle (m)
S	midpoint located between the vertices A and D
V	midpoints of the diagonals BC of the first and last hole of the first and last row

Greek letters

$\alpha, \beta, \delta, \varepsilon$	interior angles of a quadrilateral (rad)
φ	porosity (m^2 m^{-2})
ρ_x	number of threads per unit of length in the direction of weft (threads m^{-1})
ρ_y	number of threads per unit of length in the direction of warp (threads m^{-1})

Subscripts

i, j	entry in the ith row and the jth column of a matrix (porous or solid)
m, n	total number of rows and columns
x	Cartesian coordinate (points) or weft direction (parameters)
y	Cartesian coordinate (points) or warp direction (parameters)

means that the geometry of each hole is rectangular, since the threads making up the warp are usually closer together than those of the weft. The number of threads per unit length establishes the density of threads of the screen in each direction. The diameter of the threads is another variable that defines the geometry of the screen. These two parameters, taken together, determine both the dimensions of the holes and the overall porosity of the screen, i.e. the relationship between the area occupied by holes and the total area. Screen mesh size is directly related to the capacity of the net to keep insects out of the greenhouse, while the porosity is closely linked to the air exchange through porous screen. Since the porosity of these screens is usually low, they impede ventilation and reduce light transmission (Teitel, 2007).

The use of insect-proof screens reduces populations of pests inside the greenhouse (Berlinger et al., 1983, 1988, 1991, 1992; Robb and Parrella, 1988; Baker and Jones, 1989; Berlinger and Lebiush-Mordechai, 1995; Roberts et al., 1995), decreases the incidence of insect-transmitted diseases (Berlinger et al., 1983, 1991, 1992; Baker and Jones, 1989, 1990) and as a result reduces the need to apply pesticides (Berlinger et al., 1983, 1991; Robb and Parrella, 1988; Baker and Shearin, 1994; Ross and Gill, 1994; Roberts et al., 1995; Teitel, 2001). The advent of these agrotextiles is also due to the drawbacks of chemical means of pest control, such as loss of efficiency due to the swift appearance of resistant populations (Byrne and Devonshire, 1993; Berlinger et al., 2002; Gorman, 2005), high cost (Bailey, 2003), environmental impact (Bethke and Paine, 1991; Bell and Baker, 2000; Fatnassi et al., 2003), the elimination of biological control agents (Antignus, 2000), the increasingly restrictive legal framework, problems of residues in the crops (Belda and Rodríguez, 1989) and the subsequent rejection by the market (Jiménez, 1991), and the high risk factor for the workforce as a result of the toxicity of the pesticides and the time spent applying them (Cabello, 1996).

Nevertheless, insect-proof screens are not without drawbacks. Their installation on greenhouse vents considerably reduces the greenhouse's ventilation rate (Dierickx, 1998; Muñoz et al., 1999; Bartzanas et al., 2002; Linker et al., 2002; Bailey et al., 2003; Soni et al., 2005) and produces imbalances in the greenhouse microclimate with negative consequences for crop development (Kittas et al., 2002; Teitel, 2010).

Analysis of the geometric of insect-proof screens is important to characterize their effectiveness to prevent insect entry inside the greenhouse and to determine its resistance to airflow. The ability of the screens to keep insects out is determined by analysing their geometric characteristics, comparing the dimensions of the holes with the usual size of the most damaging pest species. Due to the small size of the hole, manufacturers measure the distance between adjacent threads under microscope. This procedure does not permit to get a significant number of data and is very inaccurate.

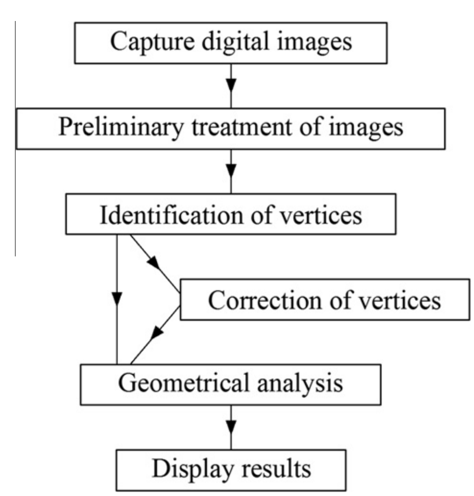

Fig. 1. Outline of analysis process of the software developed.

Hitherto no specific method was available to obtain the geometric characteristics of insect-proof screens, and so computer software (Euclides v1.4) has been designed using Visual Basic (Microsoft Corp., Version 6.0) that allows complete and precise geometric characterisation (Álvarez et al., 2006; Álvarez, 2010). Fig. 1 shows the outline of the software developed to obtain the characteristic dimensions of the insect-proof screens. The information provided by the computer software designed includes: the number of threads of weft and warp direction per unit length, the thickness of the threads, the largest circle contained in the holes, the area and the dimensions of the holes in the two main directions of the screen. Taken together these parameters allow us to estimate the validity and efficiency of the screens as a physical barrier impeding the entrance of insects. Based on the data obtained in each analysis, frequency histograms of each variable can be represented and the dispersion of the data set can be calculated to determine the uniformity of the textile. The current version of the software does not allow obtaining frequency histograms directly. The program allows exporting data to a text file that can be imported into a spreadsheet and performing all the calculations and representations that are required.

2. Materials and methods

2.1. Preparation of the samples and preliminary treatment of the images

Preparation of the sample of screen consists of inserting a small portion between two microscope slides. The microscope slide on the upper part has a drawing of a quadrilateral that defines the surface to be analysed. In this way the screen fits a plane and we ensure that the region explored is the same for all the samples analysed. The scanning range covered combining the lens of the digital camera of the microscope and the lowest power objective lens does not allow enough holes to be viewed in a single image for statistical validity of the analysis. It is therefore necessary to capture several images for each sample analysed. Incomplete columns and rows of holes will appear at the edges of the image, and so each image must overlap with the previous one.

The optimal number of pictures to take into account for the determination of the geometric characteristics of insect-proof screens depends on several factors such as the analysis purpose (a manufacturer and a researcher search very different objectives), the analysis procedure (related to the image capture device), the heterogeneity of agrotextiles (for very heterogeneous screens we will have to increase the size of the sample) or the required accuracy to the estimates.

In this work we analyze three randomly selected surfaces. The area of each surface is 1 cm^2. The number of pictures to be taken to cover the surface of 1 cm^2 depends on the overlaps that have to be considered between images (these overlaps in turn depend on the hole size). If we use the 4× objective of a microscope between 20 and 25 pictures per cm^2 are usually needed. But if another device that allows a greater field of view is used (at the expense of a smaller number of increases) greater areas can be explored with the same investment of time, although the measurement accuracy is reduced.

The microscope provides colour images in which the following tonalities can be distinguished: in screen with translucid threads (image on the left of Fig. 2) the outer part of the thread (dark colour) can be distinguished from the central part (light colour); in screen with opaque threads the whole thread appears dark; the holes between the threads are identified by their light colour. Euclides v1.4 needs to work with images in black and white. Colour images are therefore first converted into greyscale images (256 levels of grey per pixel). These images are converted into black and white images by changing the pixels with values of over 128 to white and the ones with values of under this figure to black. Thus, all the solid structure in these images of screens woven with opaque threads appears black, whereas the holes appear white. However, in the images of screens woven with translucid threads the central part of the thread also appears white. To correct this, the black and white images are transformed again to a greyscale (this action doesn't produce an apparent change) and it is used a fill-in tool to paint in a grey shade the holes (central image Fig. 2). Finally, the program turns into white all those grey pixels (holes) and the rest of the pixels are turned into black (threads). The final result is shown in the image on the right of Fig. 2.

The aim of this chromatic duality is to differentiate perfectly the regions corresponding to the holes (white pixels) from those corresponding to the threads (black pixels).

2.2. Basis of the method

The geometric analysis proposed starts with taking digital images of a sample of screen using an optical microscope. Previous calibration of the microscope allows us to know the equivalent of each pixel in metric units. The geometric basis consists of considering that each hole in the screen represents a quadrilateral as it is defined by four monofilament threads that cross over one another. Geometric characterisation of the insect-proof screens starts by obtaining the coordinates of the vertices of these quadrilaterals. Fig. 3 shows a hole located in row i and column j of the porous matrix (each hole is an element of this matrix). This hole represents a quadrilateral whose vertices are $A_{(i,j)}$, $B_{(i,j)}$, $C_{(i,j)}$ and $D_{(i,j)}$. The abscissa and ordinate of the vertex $A_{(i,j)}$ are $a_{x(i,j)}$ and $a_{y(i,j)}$, respectively. The angles of the vertices are $\alpha_{(i,j)}$, $\delta_{(i,j)}$, $\varepsilon_{(i,j)}$ and $\beta_{(i,j)}$. The software developed is able to identify these vertices by scanning the image for rows of pixels.

2.3. Geometry: general procedures

Any hole in the screen located in row i and column j of the porous matrix can be characterised using the fundamental expressions

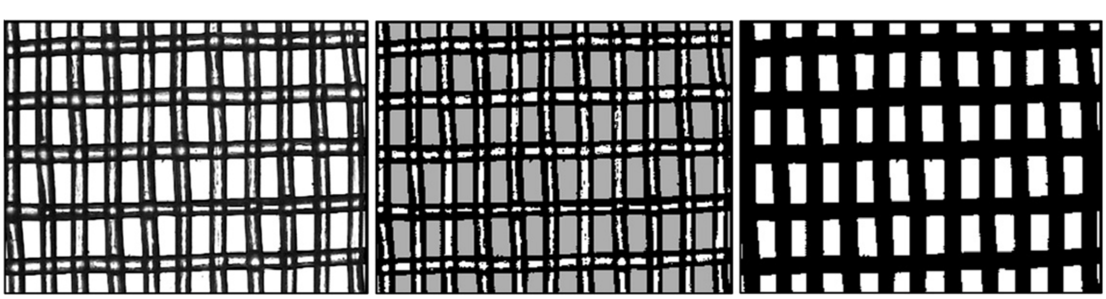

Fig. 2. Images of an insect-proof screen in colour, greyscale and black and white.

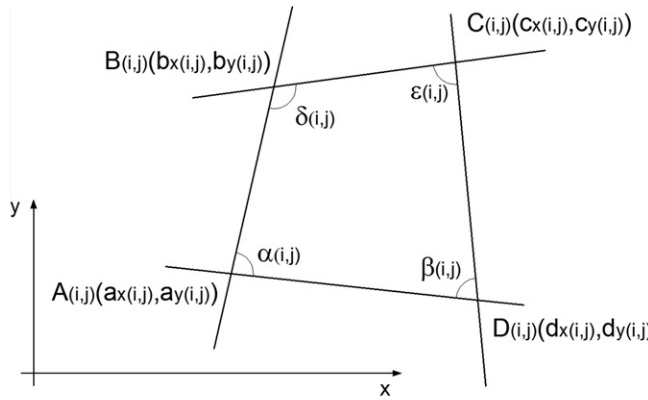

Fig. 3. Schematic representation of a hole showing the coordinates and the angles of the vertices.

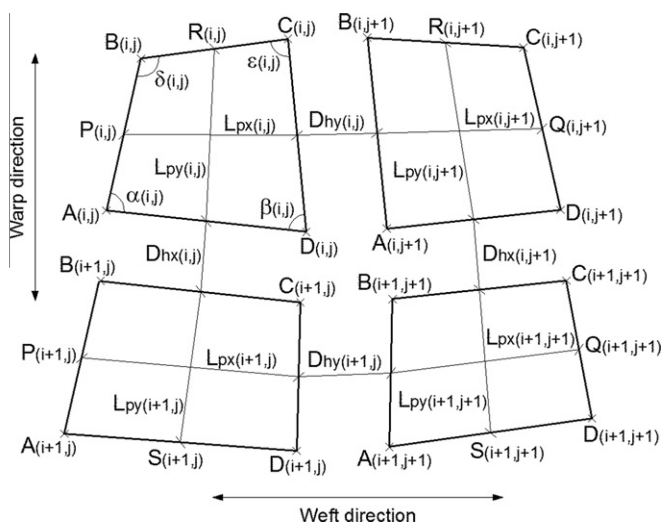

Fig. 4. Determining the dimensions of the holes and the thickness of the threads.

of plane geometry. The coordinates of point $P_{(i,j)}$ (Fig. 4) located between the vertices $A_{(i,j)}$ and $B_{(i,j)}$ (whose coordinates are defined in Fig. 3) can be obtained using the following expressions:

$$p_{x(i,j)} = \frac{a_{x(i,j)} + b_{x(i,j)}}{2} \quad (1)$$

$$p_{y(i,j)} = \frac{a_{y(i,j)} + b_{y(i,j)}}{2} \quad (2)$$

In the same way we can obtain the coordinates of point $Q_{(i,j)}$ located between vertices $C_{(i,j)}$ and $D_{(i,j)}$. The distance between $P_{(i,j)}$ and $Q_{(i,j)}$ is the distance between two points and is calculated by the following expression:

$$L_{PQ(i,j)} = \sqrt{\left(p_{x(i,j)} - q_{x(i,j)}\right)^2 + \left(p_{y(i,j)} - q_{y(i,j)}\right)^2} \quad (3)$$

In order to carry out certain calculations it is necessary to obtain the straight line that passes through two points. For instance, the slope of the straight line that includes the vertices $A_{(i,j)}$ and $C_{(i,j)}$ is obtained from the expression:

$$m_{AC(i,j)} = \frac{a_{y(i,j)} - c_{y(i,j)}}{a_{x(i,j)} - c_{x(i,j)}} \quad (4)$$

and the y-intercept of the straight line $AC_{(i,j)}$:

$$n_{AC(i,j)} = a_{y(i,j)} - m_{AC(i,j)}a_{x(i,j)} = c_{y(i,j)} - m_{AC(i,j)}c_{x(i,j)} \quad (5)$$

In other calculation procedures it proves necessary to determine the distance from a point to a line. For instance, the distance between the vertex $B_{(i,j)}$ and the line that includes the vertices $A_{(i,j)}$ and $C_{(i,j)}$ is as follows:

$$L_{B(i,j)-AC(i,j)} = \frac{\left|m_{AC(i,j)}b_{x(i,j)} - b_{y(i,j)} + n_{AC(i,j)}\right|}{\sqrt{m^2_{AC(i,j)} + 1}} \quad (6)$$

2.4. Calculation of the dimensions of the holes and the thickness of the threads

Once the images have been treated and the coordinates of the vertices of the holes are known, the characterisation of the screen is merely a geometric problem. Considering the screen as a flat surface and idealizing each hole as a quadrilateral, the dimensions of the pores in each direction is obtained as the distance between the midpoints of its opposite sides (the reason of this choice has been arbitrary). For each main direction $L_{px(i,j)}$ and $L_{py(i,j)}$ represent the characteristic dimension of the hole located in row i and column j of the porous screen, and $D_{hx(i,j)}$ and $D_{hy(i,j)}$ are the thicknesses of the threads of weft and warp, respectively, measured in row i and column j of the solid matrix (when referring to the threads, we consider one solid matrix for the weft and another one for the warp).

Given a hole located in row i column j of the set of holes, the distance between points $P_{(i,j)}$ and $Q_{(i,j)}$ is the dimension of the hole $L_{px(i,j)}$ measured in the direction of the threads of the weft. If $R_{(i,j)}$ is the midpoint between vertices $B_{(i,j)}$ and $C_{(i,j)}$, and $S_{(i,j)}$ the midpoint between vertices $A_{(i,j)}$ and $D_{(i,j)}$, the distance between these two midpoints provides the value $L_{py(i,j)}$, i.e. the mesh size measured in the direction of the warp.

Calculating the distances between points $S_{(i,j)}$ and $R_{(i+1,j)}$ we obtain the thickness of the weft thread $D_{hx(i,j)}$ measured in row i column j of the solid matrix considered for this direction of the screen. On the other hand, the distance between points $Q_{(i,j)}$ and $P_{(i,j+1)}$ is the thickness of the warp thread $D_{hy(i,j)}$ measured in row i column j of the solid matrix for the other direction.

2.5. Area of the holes

The software developed (Euclides v1.4) includes a procedure for calculating the area of the holes. The area of the hole located in row i column j of the porous matrix is obtained using the general expression for calculating the surface enclosed by a quadrilateral:

$$A_{C(i,j)} = \frac{L_{B(i,j)-AC(i,j)} + L_{D(i,j)-AC(i,j)}}{2} L_{AC(i,j)} \quad (7)$$

where, $L_{AC(i,j)}$ is the length of the diagonal of the quadrilateral joining the vertices $A_{(i,j)}$ and $C_{(i,j)}$ (distance between two points); and $L_{B(i,j)-AC(i,j)}$ and $L_{D(i,j)-AC(i,j)}$ are the distances between vertices $B_{(i,j)}$ and $D_{(i,j)}$ and the diagonal $AC_{(i,j)}$, respectively (distance between a point and a line).

2.6. Diameter of the inscribed circle

In some cases it can be assumed that the cross-section of the body of greenhouse pests is approximately circular. In these cases it is of particular interest to calculate the diameter of the largest circle that can be inscribed inside a hole of the insect-proof screen. The diameter calculated will also be a parameter which will be considered in the decision on which type of screen to install in the greenhouse vents, depending on the species of insects which are to be kept out. However, the ability of insects to pass through an opening cannot be predicted only according to the insects thoracic width and the hole size (Bethke and Paine, 1991). Therefore, it's necessary to relate the dimensions of the holes and the ability of the insects. Future researches will have to solve this problem.

In order to calculate the circle of largest diameter that can be inscribed inside a hole of the screen, the reasoning has been as follows: if each of the sides of quadrilateral is eliminated in turn, four open polygons are obtained. For each of these a circle can be drawn in such a way that the three sides of the polygon (or the straight lines these sides included in) are tangents to it. If we now consider the side that was previously eliminated, it could be that the straight line that includes this side is outside the circle, a tangent or a secant (in the first two cases the circle would be considered inside the polygon). If the line is a tangent, the four possible circles are similar. If there is no tangency, of the four possible circles two will not come into contact with the line considered. These two circles may be equal (when the quadrilateral is a parallelogram), and so either of them is the desired one. On the other hand, they may present different diameters, and in this case we should choose the one with the greatest diameter.

In order to solve mathematically the approach described above, given a hole located in row i column j of the porous matrix, we must first determine the equations of the lines that include the sides of the quadrilaterals. We should bear in mind the possibility that any of the lines that pass through the vertices $AB_{(i,j)}$ or $CD_{(i,j)}$ may be a vertical asymptote. As the slopes of the lines are known, the angles of the quadrilateral's vertices can be calculated and the equations of the bisectors can be obtained. On solving the intersection between the bisector of angle $\alpha_{(i,j)}$ and the bisector of angle $\delta_{(i,j)}$ we obtain the coordinates of the centre of one of the four circles $O_{1(i,j)}$. The centres of the other three circles are determined by solving the intersections of the remaining consecutive bisectors of the quadrilateral.

The radius $r_{(i,j)}$ of the circles inscribed in the quadrilateral can be calculated as the distance between a point and a line (the distance between its centre and one of the tangents). In the same way we determine the distances $d_{(i,j)}$ between the centres of the circles and the sides that enclose, in each case, to the open polygon. A circle is said to be inside the quadrilateral when the length of the radius is less than or equal to the distance measured between its centre and the side that closes the open polygon ($r_{(i,j)} \leqslant d_{(i,j)}$). Finally, the inner circle of largest diameter is chosen.

2.7. Geometry of the holes

One quality parameter of any insect-proof screen is related to the uniformity of the fabric. Uniformity of the hole size is a fundamental aspect to ensure that the screen fulfils its purpose satisfactorily. The dimension of the holes must be established according to the smallest species of insects to be kept out of the greenhouse. It is therefore essential that these dimensions be maintained over the whole surface of the screen.

An ideal screen would maintain the threads perfectly parallel and equidistant in each direction, ensuring that all the holes are regular parallelograms. However, the manufacturing process of the textile is conditioned by many variables, some of which depend on the manufacture of the threads themselves and on the technological level of the looms, and so the desired uniformity is not always achieved. Indeed, the manufacture of the textile is conditioned by many parameters which are difficult to control and which depend on the expertise and know-how of the manufacturer.

The geometry of the holes can be determined by analysing either the slope of the lines which include the sides of the quadrilaterals or the angles of the vertices. Finally, the latter option was chosen, as it avoids the complication that might appear if sides $AB_{(i,j)}$ or $CD_{(i,j)}$ belonged to a vertical asymptote. In order to study the geometry of the holes, Euclides v1.4 uses a loop that examines all the holes in the screen, checking the relationships between their angles: the quadrilateral considered is treated as a parallelogram when two opposite angles are equal; if this is not the case, but a pair of consecutive angles adds up to 180° it is treated as a trapezium; and finally, the quadrilateral is a trapezoid if neither of the above conditions is fulfilled.

2.8. Number of threads per unit length

The number of threads per unit of length (threads cm^{-1}) in the directions of weft ρ_x and warp ρ_y of the screen has been calculated using the following expressions:

$$\rho_x = \frac{1}{l_{py} + d_{hx}} \tag{8}$$

$$\rho_y = \frac{1}{l_{px} + d_{hy}} \tag{9}$$

Given a porous matrix with m rows and n columns, the value d_{hx} represents the mean thickness of the weft thread measured in the direction of the line that includes midpoint $R_{(1,j)}$ in side $BC_{(1,j)}$ of the first hole in a given column and midpoint $S_{(m,j)}$ in side $AD_{(m,j)}$ of the last hole in the same column (Fig. 4). Following the same procedure for all the columns of holes of the sample analysed, we obtain a set of data whose mean value allows us to know value d_{hx}. Dimension l_{py} is the mean mesh size measured in the direction of the lines calculated to obtain d_{hx}.

If we now consider rows of holes instead of columns, we can obtain lines that pass through midpoint $P_{(i,1)}$ in side $AB_{(i,1)}$ of the first hole of a given row and midpoint $Q_{(i,n)}$ in side $CD_{(i,n)}$ of the last hole in the same row. Repeating the operation for all the rows of holes, we obtain a set of data that allow us to calculate the mean thickness of threads d_{hy} and the mean mesh size l_{px} in the direction of these lines.

Obviously, these dimensions would only coincide with those described in the section 2.4 ‘‘Calculation of the dimensions of the holes and the thickness of the threads’’ ($L_{px} = l_{px}, L_{py} = l_{py}, D_{hx} = d_{hx}$ and $D_{hy} = d_{hy}$) if the screen were completely regular. In general we can say that $L_{px} \approx l_{px}, L_{py} \approx l_{py}, D_{hx} \approx d_{hx}$ and $D_{hy} \approx d_{hy}$.

2.9. Calculating porosity

The separation of the threads that make up the fabric of an insect-proof screen defines a porous matrix formed by rows and columns of holes. This set of threads and holes form a porous material and constitutes an object which may be seen flat from the macroscopic point of view. An important property of these materials is its porosity defined as the surface area occupied by holes A_p with regard to the total surface area A_t considered:

$$\varphi = \frac{A_p}{A_t} = \frac{L_{px}L_{py}}{(L_{px} + D_{hy})(L_{py} + D_{hx})} \tag{10}$$

Considering a digital image where the white pixels represent the porous surface area and the black pixels represent the solid surface area, obtaining the porosity is reduced to calculate the relationship between the number of white pixels A_p with regard to total number of pixels A_t. However, to obtain a more accurate value of the porosity of screens it is essential to make a correct choice of the total surface area considered. This reference surface area A_t must be chosen so as to ensure a proportional allocation between the porous surface area and the solid surface area. Proportional allocation follows the criteria that the surface area of every hole of the screen is related to a reference surface area defined by the longitudinal axes of the threads that define that hole. Applying this idea to the image in Fig. 5, the total surface area is represented by the blue shaded surface area and is obtained by calculating the midpoints V of the BD diagonals of the first and last hole of the first and last rows. In general, the quadrilateral defined by the points

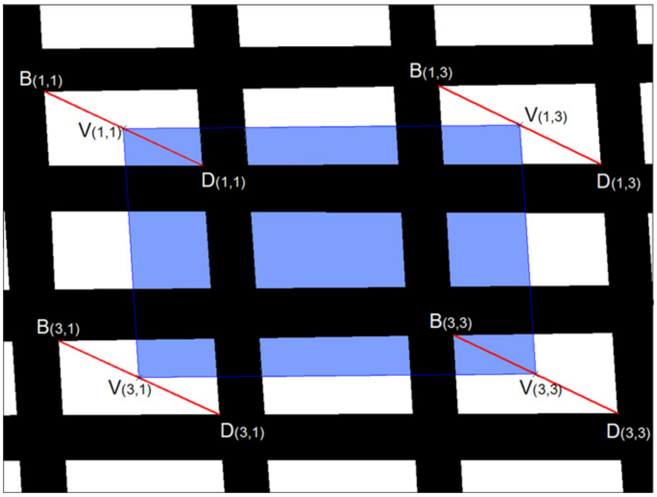

Fig. 5. Obtaining the porosity of the screen.

$V_{(1,1)}, V_{(1,n)}, V_{(m,1)}$ and $V_{(m,n)}$ represents the total surface area A_t and its surface area can be calculated using the Eq. (7). Once defined the total surface area, Euclides v1.4, obtains the porous surface area A_p within that reference surface area. Finally, the relationship between both surface areas allows to obtain the value of porosity.

3. Results and discussion

3.1. Synthesis of the software developed

The application developed to calculate the geometric characteristics of the insect-proof screens consists of 4 forms, 2 standard code modules, 9 main menus, 22 submenu items that allow to access all the options the programme offers, 6 picture boxes, 2 scroll bars, 3 common dialogs, 1 label that asks the user for information in different procedures of the image process analysis, 1 progress bar that provides information on the progress of the operation identifying the vertices, 1 status bar that shows the state of the analysis process, 1 image control that shows a region of the image in the form of correction of vertices, 1 shape control indicating the pixel where a vertex will be aggregated, 1 command button, 1 flexgrid table to show results, 6 message dialog boxes offering information and results and 3 input dialog boxes to collect information from the user. The software code responds to 40 events, including different actions with the mouse or modifications in the state of different controls.

3.2. Identification of vertices

In this phase of the analysis process, Euclides v1.4 scans the image marking on it the vertices identified. The image is scanned row by row of pixels to compare, for each pixel, the colour of the surrounding pixels using a pattern incorporated into the programme to decide whether the pixel analysed corresponds to a vertex. This was one of the most complex development phases of the software, as it was necessary to find a pattern that was sufficiently simple to maintain the identification process within a reasonable time limit. The problem of working with simple patterns is that they are not able to contemplate the wide variety of combinations of black and white of the pixels around the vertices, and therefore their percentage of success is low. Finally, it was possible to devise a pattern that is both simple and able to achieve a high percentage of success. For each pixel this pattern needs to analyse sixteen pixels close to the point studied. Fig. 6 is a graphic representation, indicating with Cartesian coordinates the pattern used according to

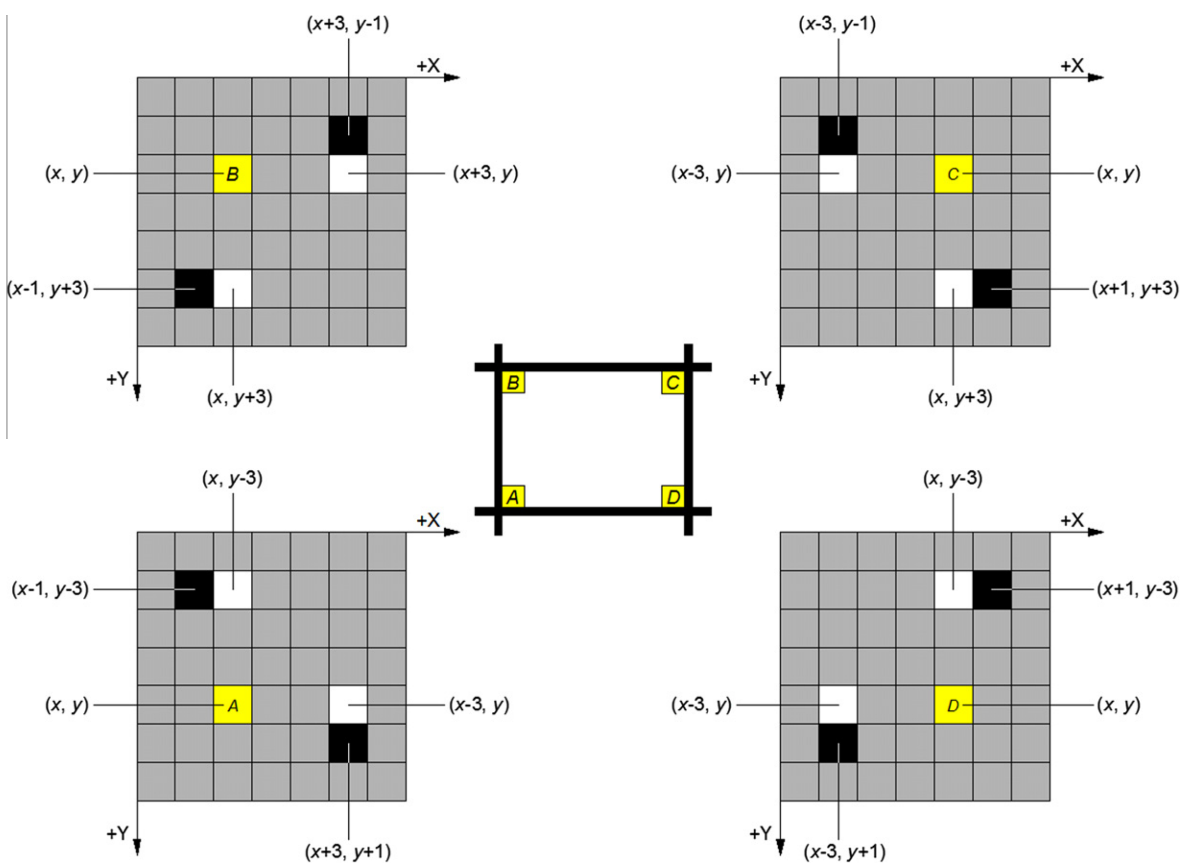

Fig. 6. Diagram of the pattern used to identify vertices.

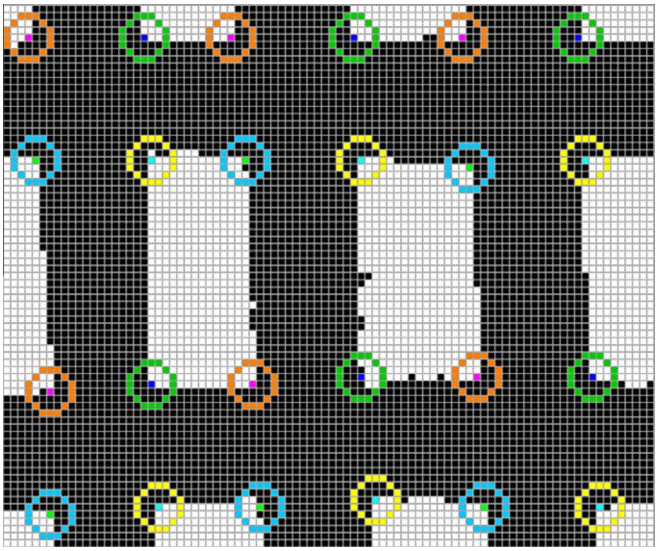

Fig. 7. Enlarged detail of the result obtained after identifying vertices.

the position of the pixel considered. In the centre of the figure a hole is represented, defined by the crossing of four threads; the vertices of this hole (pixels) are marked by squares with a yellow background. The grid marked in Fig. 6 symbolizes the pixels in which the image is divided.

For example, given a pixel of coordinates (x,y), Euclides v1.4 will decide that this is a $B_{(i,j)}$ vertex (situated in the upper left-hand corner of the hole) only if the neighbouring pixels $(x+3,y)$ and $(x,y+3)$ are white and the pixels of coordinates $(x+3,y-1)$ and $(x-1,y+3)$ are black (Fig. 6). With this simple pattern the identification of vertices can be carried out in a few seconds and with a high degree of success.

Once the vertices have been identified, it can be observed in the image that Euclides v1.4 has drawn circles whose centres coincide with the vertices detected (Fig. 7). These circles have different colours depending on the vertex considered. This colour code assigned to the circles is merely to inform the user. Euclides v1.4 uses another colour code that will be interpreted in a later operation to identify the centre of the circles, i.e. the pixel that coincides with the vertex identified. This code also uses a different colour for each vertex, although these colours do not coincide with those used to draw the circles.

3.3. Detection of errors in the identification of vertices

During the identification of vertices two types of error may occur: one occurs when the software is unable to identify a vertex or it is marked in an incorrect place; the other type of error seldom occurs, and it is when the programme identifies a vertex incorrectly, i.e. the software confuses one vertex with another one. For example, it may confuse a vertex $A_{(i,j)}$ with a vertex $C_{(i,j)}$ due to a strange arrangement of pixels around a vertex. Each vertex identified is marked with a circle and each circle has a different colour (green, yellow, sky-blue, orange) depending on the vertex ($A_{(i,j)}$, $B_{(i,j)}$, $C_{(i,j)}$ and $D_{(i,j)}$) it represents. The programme reports when an error occurs and the user can locate the vertex misidentified by the colour of the circles that the software uses to highlight the vertices detected (Fig. 7).

From this moment on, the image is reduced to a set of coloured, disperse pixels for the programme. These pixels are those that were marked at the points where the vertices were identified. Therefore, it ignores the black and white pixels as well as the coloured ones corresponding to the circles that were drawn around the vertices to inform the user of their location. Therefore the colour code used to mark the vertices is unique and does not coincide with any other colour used on the image.

In order to detect the first type of error the software carries out the following verification process. On the one hand it counts the number of vertices, and on the other it calculates this amount from the number of rows and columns of holes, comparing both values.

To detect the second type of error, i.e. those that imply incorrect identification of a vertex, Euclides v1.4 makes a horizontal scan of the rows of pixels of the image analysed. The software's procedure responsible for detecting this type of error consists of counting separately each set of vertices (vertices *A*, *B*, *C* and *D*). Euclides v1.4 issues a warning if there is a set of vertices with one or more vertices in excess and another set of vertices with a shortage of one or more vertices.

3.4. Correction of vertices

The presence of dirt among the threads of the screen is one of the reasons that can induce Euclides v1.4 to identify a vertex in an incorrect position. If an error has occurred in the identification of vertices it can be corrected. The image is loaded in a second form and is enlarged by a factor of four. A square frame appears in the centre limiting a surface equal to a pixel; this square frame defines the position where a vertex will be aggregated or eliminated (Fig. 8).

The elimination of a vertex is performed by restoring the original colour of the pixels in the position that the undesired vertex has. To add a vertex, the cursor of the mouse must be placed over the corresponding pixel. As this proves fundamental for later operations, the programme should find out what type of vertex must add ($A_{(i,j)}$, $B_{(i,j)}$, $C_{(i,j)}$ or $D_{(i,j)}$). To this end, Euclides v1.4 studies four sets of three pixels (Fig. 9) situated on two lines with slopes of 45° and 135°, traced from the pixel chosen. Along these lines the programme studies the colour of the pixels located at distances of 4, 8 and 10 pixels from the selected pixel (these values can be changed depending on thickness of the threads). Three of these sets will be made up of black pixels because they correspond with threads, while one will contain at least one white pixel (usually all three pixels in this set will be white because they correspond with a hole). Euclides v1.4 is able to recognize the vertex ($A_{(i,j)}$, $B_{(i,j)}$, $C_{(i,j)}$

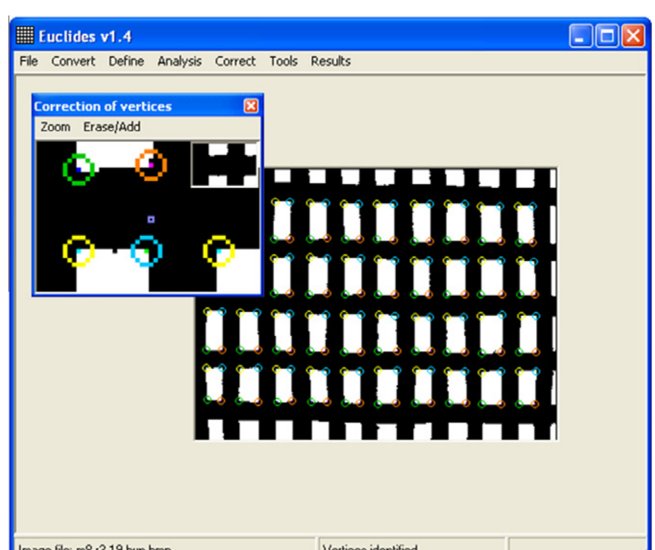

Fig. 8. Correction of vertices.

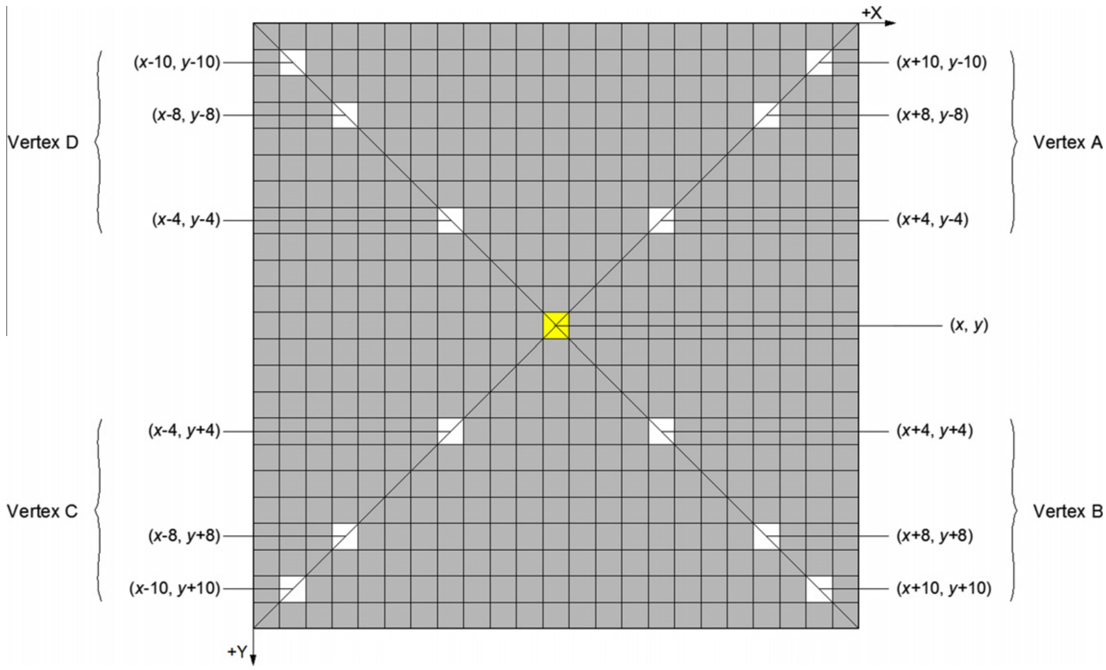

Fig. 9. Pattern used in the operation to aggregate vertices.

or $D_{(i,j)}$) according to the position of the set of white pixels in relation to the sets of black pixels (Fig. 9).

3.5. Coordinates of the vertices

Once the vertices are correctly marked on the image, and before commencing the geometric analysis, the coordinates of the vertices must be obtained, sorted and stored. To obtain the coordinates of the vertices the programme carries out a scan along the rows of pixels on the analysed image in which Euclides v1.4 only considers the pixels marked as vertices. The scan of the rows of pixels usually means that the coordinates of the vertices are obtained in a disorderly fashion with respect to the column of the porous matrix in which they belong, as it is normal that the vertices are not aligned horizontally. This problem has been solved by using the algorithm known as *insertion sort*. This algorithm consists of comparing the abscissas of the vertices two by two maintaining their position when the abscissa of the first point is less than that of the second one, or modifying it when this is not the case. The final result is a set of data that contains the coordinates of the vertices of each hole in order. It is therefore possible to locate each vertex according to the row and column of the hole to which it belongs.

3.6. Correction of coordinates

A very important aspect is related to the values of the coordinates of the pixels that give programming applications. Really, a pixel is not a point but rather a small surface: the minimum graphic unit of measurement. Consequently, on requesting the coordinate of vertex using the code, the programme gives the position of the centre of the pixel. This implies that the parameters related to the holes are underestimated, and on the other hand the thickness of the threads is overestimated (Fig. 10). It is therefore necessary to carry out a correction of all the data pairs in order that the point they define is the one of the vertices of the pixel and not its centre.

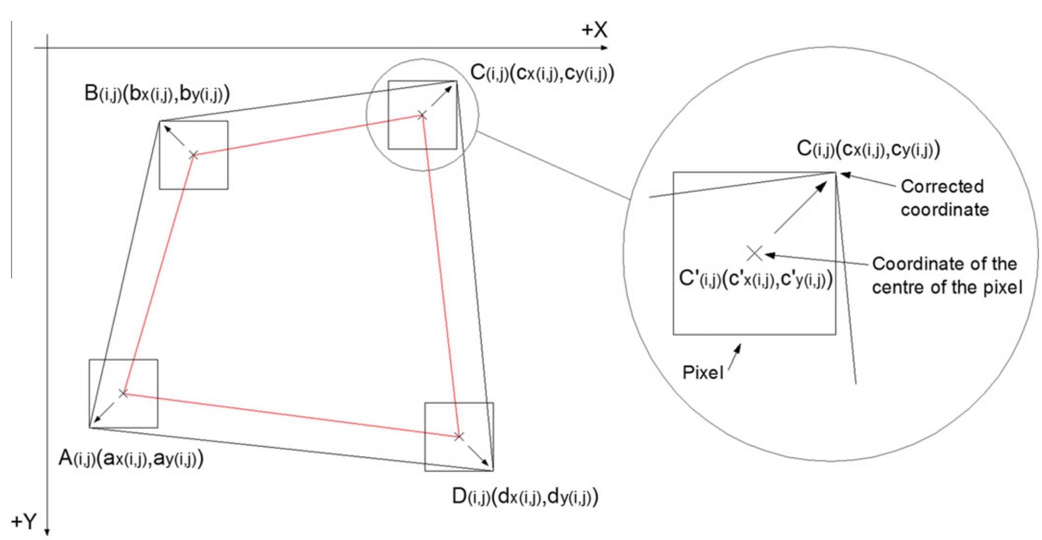

Fig. 10. The correction of coordinates implies moving them from the centre of the pixel to one of the vertices.

Table 1
Operations allow correcting the coordinates of the vertices.

Vertex	Abscissa of the pixel	Ordinate of the pixel
$A_{(i,j)}$	$a_{x(i,j)} = a'_{x(i,j)} - 0.5$	$a_{y(i,j)} = -a'_{y(i,j)} - 0.5$
$B_{(i,j)}$	$b_{x(i,j)} = b'_{x(i,j)} - 0.5$	$b_{y(i,j)} = -b'_{y(i,j)} + 0.5$
$C_{(i,j)}$	$c_{x(i,j)} = c'_{x(i,j)} + 0.5$	$c_{y(i,j)} = -c'_{y(i,j)} + 0.5$
$D_{(i,j)}$	$d_{x(i,j)} = d'_{x(i,j)} + 0.5$	$d_{y(i,j)} = -d'_{y(i,j)} - 0.5$

Table 1 shows the expressions that permit the correction of the vertices. With these expressions the point considered is transferred from the centre of the pixel to the corresponding vertex. For this purpose we bear in mind that the origin of the coordinate system coincides with the upper left-hand corner of the images. The sign of the ordinates has also been corrected, as the programming applications assign positive values to the *y*-axis pointing down.

Once the coordinates of the vertices of the holes have been corrected, the programme converts the units to work with micrometres instead of pixels. To do so it simply multiplies by the factor that defines the equivalence of a pixel in metric units. This will depend on the device used to obtain the images.

3.7. Viewing results

The results generated by the programme after the analysis can be viewed directly or exported to a text file. The results can be viewed in the programme itself on a diagram of the screen showing the number of threads per unit length of the net analysed, the porosity and the mean values of the dimensions and area of the holes, thickness of the threads and diameter of the largest circle inscribed inside the holes (Fig. 11). The results can also be viewed in tabulated form. If the data are exported to a text file for later treatment, on analysing a sequence of images belonging to the same sample, the programme allows the results of each of the images analysed to be aggregated to the same text file, thus enabling the user to carry out a single treatment of the data set.

With this collection of data the mean values can be obtained for the dimensions of the holes (L_{px} and L_{py}) and the thickness of the threads (D_{hx} and D_{hy}) in each of the main direction of the screen; in addition, from the data obtained in each analysis, frequency histograms of each variable can be drawn and the dispersion of the data set can be analysed to determine the uniformity of the textile and to detect manufacturing faults.

3.8. Contrasting the results: measurements of insect-proof screens

To analyse the reliability of the software developed, a manufacturer of renown was commissioned to produce five agrotextiles with pre-established characteristics, since the information of the manufactured products is not contrasted. For this purpose the threads of the screen, of known thicknesses, were also manufactured *ex professo*. The number of threads of warp direction per unit length of all the screens was the same (31 threads cm^{-1}), as to vary this parameter proves very costly. On the other hand, the number of threads of weft direction varied in the different screens.

Three randomly chosen samples were taken from each screen, and for each one a surface of 1 cm^2 was analysed. The design values

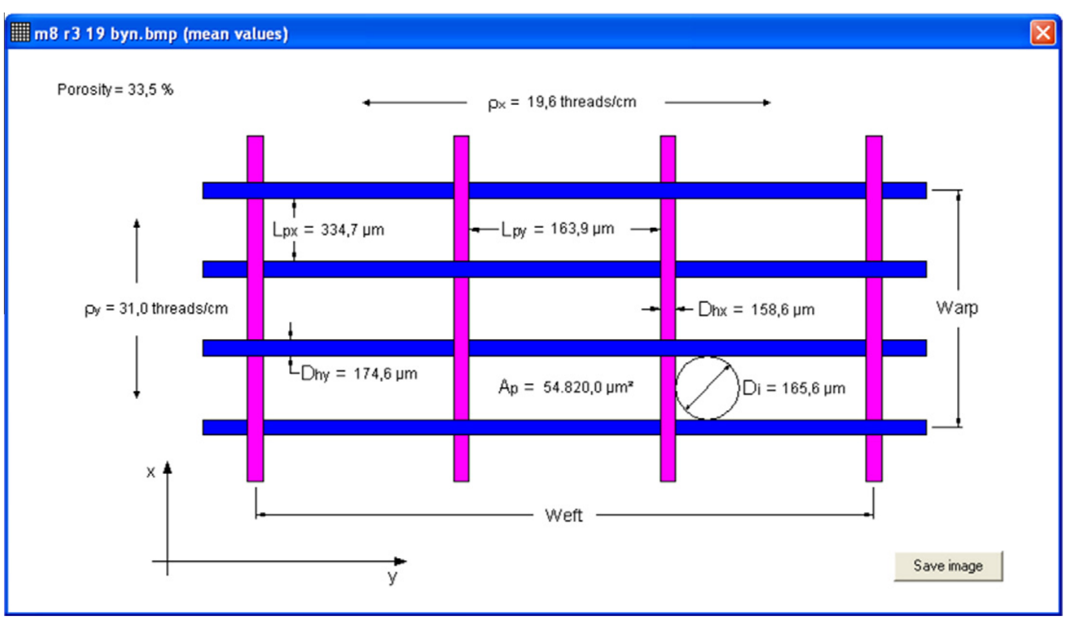

Fig. 11. Viewing results (mean values).

Table 2
Design values and measurements taken by the software of the manufactured screens.

Screen	Design values			Measured values		
	$\rho_x \times \rho_y$ (threads cm^{-2})	D_{hx} (µm)	D_{hy} (µm)	$\rho_x \times \rho_y$ (threads cm^{-2})	$D_{hx} \pm \sigma$ (µm)	$D_{hy} \pm \sigma$ (µm)
1	15 × 31	110	110	15.2 × 30.2	110.5 ± 4.2	109.9 ± 5.1
2	18 × 31	110	110	18.6 × 31.3	110.6 ± 4.3	110.2 ± 4.3
3	16 × 31	110	160	16.2 × 30.3	108.6 ± 4.4	162.6 ± 5.2
4	16 × 31	160	160	16.1 × 30.8	163.1 ± 5.3	162.8 ± 6.3
5	14 × 31	160	160	14.2 × 30.7	159.8 ± 5.7	163.5 ± 6.5

Table 3
Calculated and measured values of the manufactured screens.

Screen	Calculated values			Measured values			Number of holes
	L_{px} (μm)	L_{py} (μm)	φ (%)	$L_{px} \pm \sigma$ (μm)	$L_{py} \pm \sigma$ (μm)	φ (%)	
1	221.2	547.4	55.6	221.6 ± 19.6	548.8 ± 8.7	55.6	1971
2	209.3	427.0	52.0	209.0 ± 12.0	427.7 ± 7.7	52.0	2192
3	167.4	508.7	41.8	168.1 ± 10.7	510.1 ± 34.1	42.0	1947
4	161.9	458.0	36.8	162.2 ± 10.6	458.4 ± 17.8	36.8	2007
5	162.2	544.4	38.5	162.6 ± 10.8	540.6 ± 17.5	38.5	1986

and the measurements of thread thickness and number of threads per unit length taken by the software developed are shown in Table 2.

The sensitivity of the measures made on microscopic images corresponds to one pixel and the calibration of the microscope for the lens used to take the images (4×) establishes a relationship of 10.5 μm pixel^{-1}. The values measured by the software developed (Table 2) prove that the manufacturer succeeded in preparing the five screens according to the design stipulations. The maximum difference in the number of threads per unit length occurred in screen number 1 with a value of 0.8 threads cm^{-1} less in the direction of the warp. As for the thickness of the threads, the maximum difference found between the valued of the design and the measurement taken was 3.5 μm. The differences found for both variables are small and to be expected, as in the manufacturing process of the threads it is common not to achieve the exact measurement desired, and it is also usual that the thickness of the thread is not maintain perfectly constant; achieving an exact number of threads per unit length on a loom is highly complex, as it depends on many variables (contraction of the threads, technology used, expertise of the manufacturer, etc.).

From the measured values of number of threads per unit length and thickness (Table 2) we can calculate the mean dimensions of the holes and porosity of the screen (Table 3) obtained with the Eqs. (8)–(10). Comparison of the calculated and measured values allows us to contrast the reliability of the software developed. The mean values of the measured and calculated variables are shown in Table 3. The discrepancies between the two groups of values reveals that the greatest differences in the dimension of the holes in the direction of the weft and warp are 0.7 and 3.8 μm, respectively (well below the sensitivity of the measurement method); regarding porosity the difference between the values calculated using manufacturer's data and measured values is 0.2%. These data constitute a clear indication of the reliability of the measurement method.

As regards the percentage of success of the pattern used to identify the vertices, the following results were obtained: 40,412 vertices studied, obtaining 1.14% errors, mainly due to the presence of dirt on the screen; of that percentage 0.13% corresponds to vertices that were not detected by the pattern, and only 0.01% were vertices that were identified incorrectly, i.e. the pattern identified a vertex in the place of another one. All these errors were correctly detected by the procedures described above.

4. Conclusions

Novel software has been developed to obtain the characteristic dimensions and the porosity of insect-proof screens with great accuracy and in times that allow analysis series of a great number of samples. The accuracy of the characteristic measurements of insect-proof screens is essential both to study their capacity for keeping out pests and to apply models that explain their aerodynamic behaviour. Published research papers that examine these aspects of the screens usually do not specify the method of measurement used to obtain the geometric characteristics of the screen nor the number of data used to calculate the mean values considered.

The results obtained by Euclides v1.4 cannot be contrasted since there is no alternative method that allows the geometric parameters of insect-proof screens to be calculated. For this reason, five screens with pre-established characteristics were manufactured to analyse the reliability of the method. The results have been excellent and the obtained values prove the accuracy of the measurements.

Bearing in mind the importance of calculating porosity in the aerodynamic study of insect-proof screens, the procedure incorporated in the software developed allows the user to obtain a highly accurate value of this parameter as it performs a proportional allocation between the porous surface area and corresponding solid matrix in such a way that each hole of the screen is related to a reference surface area defined by the longitudinal axes of the threads that define the hole (or the proportional part if the hole is incomplete). In calculating porosity, generic programmes count the pixels corresponding to holes and the total pixels of the digital image and calculate the relationship between both values.

There is no standard that allows us to certify the quality of insect-proof screens. The software developed here provides manufacturers with opportunity to carry out quality controls on their products, to offer farmers detailed information to enable them to choose a textile according to their requirements, and it is also a tool which, in the near future, will allow standardised norms to be applied in the market of insect-proof screens.

Acknowledgements

This work was founded by projects AGL2010-22284-C03-01 of Ministerio de Ciencia e Innovación of Spain and P09-AGR-4593 of Junta de Andalucía.

References

Álvarez, A.J., 2010. Estudio de las características geométricas y del comportamiento aerodinámico de las mallas antiinsectos utilizadas en los invernaderos como medida de protección vegetal. Doctoral Thesis. Almería University, Editorial Universidad de Almería (in Spanish).

Álvarez, A.J., Valera, D.L., Molina-Aiz, F.D., 2006. A method for the analysis of the geometric characteristics of protection screens. Acta Horticulturae (ISHS) 719, 557–564.

Antignus, Y., 2000. Manipulation of wavelength-dependent behaviour of insects: an IPM tool to impede insects and restrict epidemics of insect-borne viruses. Virus Research 71, 213–220.

Bailey, B., 2003. Screens stop insects but slow airflow. Fruit & Vegetable Technology 3 (2), 6–8.

Bailey, B.J., Montero, J.I., Pérez Parra, J., Robertson, A.P., Baeza, E., Kamaruddin, R., 2003. Airflow resistance of greenhouse ventilators with and without insect screens. Biosystems Engineering 86, 217–220.

Baker, J.R., Jones, R.K., 1989. Screening as part of insect and disease management in the greenhouse. N.C. Flower Growers' Bulletin 34, 1–9.

Baker, J.R., Jones, R.K., 1990. An update on screening as part of insect and disease management in the greenhouse. N.C. Flower Growers' Bulletin 35, 1–3.

Baker, J.R., Shearin, E.A., 1994. An update on screening for the exclusion of insect pest. N.C. Flower Growers' Bulletin 39 (2), 6–11.

Bartzanas, T., Boulard, T., Kittas, C., 2002. Numerical simulation of the airflow and temperature distribution in a tunnel greenhouse equipped with insect-proof screen in the openings. Computers and Electronics in Agriculture 34, 207–221.

Belda, J.E., Rodríguez, M.D., 1989. Control de trips (*Frankliniella occidentalis*) en cultivos hortícolas protegidos. Hortícolas 10, 21–31 (in Spanish).

Bell, M.L., Baker, J.R., 2000. Comparison of greenhouse screening materials for excluding whitefly (*Homoptera*: *Aleyrodidae*) and thrips (*Thysanoptera*: *Thripidae*). Journal of Economic Entomology 93 (3), 800–804.

Berlinger, M.J., Lebiush-Mordechai, S., 1995. Physical methods for the control of *Bemisia*. In: Gerling, D., Mayer, R.T. (Eds.), *Bemisia* 1995: Taxonomy, Biology, Damage, Control and Management. Intercept Ltd., Andover, UK, pp. 617–634.

Berlinger, M.J., Gol'berg, A.M., Dahan, R., Cohen, S., 1983. The use of plastic covering to prevent the spread of tomato yellow leaf curl virus in greenhouses. Hassadeh 63, 1862–1865.

Berlinger, M.J., Dahan, R., Mordechai, S., 1988. Integrated pest management of organically grown tomatoes in Israel. Applied Agricultural Research 3, 233–238.

Berlinger, M.J., Lebiush-Mordechi, S., Leeper, A., 1991. Application of screens to prevent whitefly penetration into greenhouses in the Mediterranean basin. Bulletin of International Organisation for Biological and Integrated Control of Noxious Animals and Plants (IOBC) / West Palaearctic Regional Section (WPRS) XIV (5), 105–110.

Berlinger, M.J., Leblush-Mordechl, S., Fridja, D., Mor, N., 1992. The effect of types of greenhouse screens on the presence of western flower thrips: a preliminary study. OILB-SROP Bulletin 16 (2), 13–19.

Berlinger, M.J., Taylor, R.A.J., Lebiush-Mordechi, S., Shalhevet, S., Spharim, I., 2002. Efficiency of insect exclusion screens for preventing whitefly transmission of tomato yellow leaf curl virus of tomatoes in Israel. Bulletin of Entomological Research 92, 367–373.

Bethke, J.A., Paine, T.D., 1991. Screen hole size and barriers for exclusion on insect pest of glasshouse crops. J. Entomol. Sci. 26, 169–177.

Brown, S.L., Brown, J.E., 1992. Effect of plastic mulch color and insecticides on thrips population and damage to tomato. HortTechnology 2 (2), 208–211.

Byrne, F.J., Devonshire, A.L., 1993. Insensitive acetyl cholinesterase and esterase polymorphism in susceptible and resistant populations of the tobacco whitefly *Bemisia tabaci* (Genn.). Pesticide Biochemistry and Physiology 45, 34–42.

Cabello, T., 1996. Utilización de pesticidas en cultivos en invernaderos del sur de España y análisis de los riesgos toxicológicos y medio ambientales. Phytoma España 75, 11–19 (in Spanish).

Dierickx, W., 1998. Flow reduction of synthetic screens obtained with both a water and airflow apparatus. Journal of Agricultural Engineering Research 71, 67–73.

Fatnassi, H., Boulard, T., Bouirden, L., 2003. Simulation of climatic conditions in full-scale greenhouse fitted with insect-proof screens. Agricultural and forest meteorology 118, 97–111.

Gorman, K., 2005. Resistencia de la mosca blanca a los insecticidas, *Bemisia tabaci* y *Trialeurodes vaporariorum*. Phytoma España 173, 43–44 (in Spanish).

Hussey, N.W., 1985. Whitefly control by parasites. In: Hussey, N.W., Scopes, N. (Eds.), Biological Control: The Glasshouse Experience. Academic Press, San Diego, pp. 104–115.

Jiménez, R., 1991. Repercusión económica de las enfermedades sobre los cultivos intensivos forzados. Phytoma España 31, 51–54 (in Spanish).

Kittas, C., Boulard, T., Bartzanas, T., Katsoulas, N., Mermier, M., 2002. Influence of an insect screen on greenhouse ventilation. Transactions of the ASAE 45 (4), 1083–1090.

Lacasa, A., Contreras, J., 1993. Comportamiento de *Frankliniella occidentalis* en la transmisión del virus del bronceado del tomate: planteamientos para su control en cultivos hortícolas. Phytoma España 50, 33–39 (in Spanish).

Linker, R., Tarnopolsky, M., Seginer, I., 2002. Increased resistance to flow and temperature-rise resulting from dust accumulation on greenhouse insect-proof screens. En: ASAE Annual International Meeting, Chicago, USA, 28–31 de Julio, p. 9.

McLean, G.D., Garret, R.G., Ruesink, W.G., 1986. Plant Virus Epidemics. Academic Press, Orlando, FL, pp. 550.

Muñoz, P., Montero, J.I., Antón, A., Giuffrida, F., 1999. Effect of insect-proof screens and roof openings on greenhouse ventilation. Journal of Agricultural Engineering Research 73, 171–178.

Robb, K.L., Parrella, M.P. 1988. *Chemical and no-chemical control of western flower thrips*. In: Proceedings, Fourth Conference of Insect and Disease Management on Ornamentals. Society of American Florists, Kansas City, MO, pp. 94–103.

Roberts, W.J., Vasvary, L., Kania, S., 1995. Screening for insect control in mechanically ventilated greenhouses. ASAE Paper No. 954541.

Ross, D.S., Gill, S.A., 1994. Insect screening for greenhouses. Information Facts, University of Maryland at College Park, FACTS 186, p. 21.

Smith, K.M., 1972. Plant Virus Diseases. Academic Press, NY, p. 684.

Soni, P., Salokhe, V.M., Tantau, H.J., 2005. Effect of screen mesh size on vertical temperature distribution in naturally ventilated tropical greenhouses. Biosystems Engineering 92 (4), 469–482.

Teitel, M., 2001. The effect of insect-proof screens in roof openings on greenhouse microclimate. Agricultural and Forest Meteorology 110, 13–25.

Teitel, M., 2007. The effect of screened openings on greenhouse microclimate. Agricultural and Forest Meteorology 143, 159–175.

Teitel, M., 2010. Using computational fluid dynamics simulations to determine pressure drops on woven screens. Biosystems Engineering 105, 172–179.